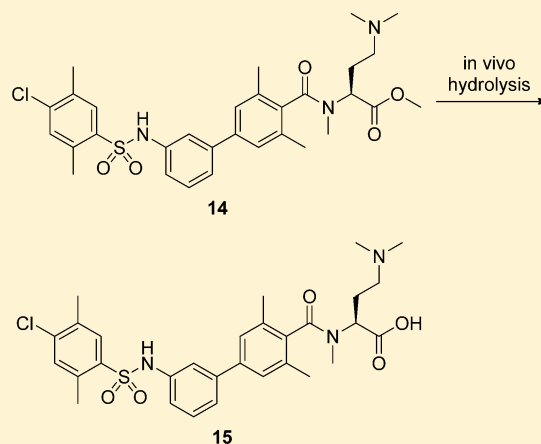# An Oral Sphingosine 1-Phosphate Receptor 1 (S1P$_1$) Antagonist Prodrug with Efficacy in Vivo: Discovery, Synthesis, and Evaluation

Daniela Angst,* Philipp Janser, Jean Quancard, Peter Buehlmayer, Frederic Berst, Lukas Oberer, Christian Beerli, Markus Streiff, Charles Pally, Rene Hersperger, Christian Bruns, Frederic Bassilana, and Birgit Bollbuck

Novartis Pharma AG, Novartis Institutes for BioMedical Research, 4002 Basel, Switzerland

ⓢ **Supporting Information**

ABSTRACT: A prodrug approach to optimize the oral exposure of a series of sphingosine 1-phosphate receptor 1 (S1P$_1$) antagonists for chronic efficacy studies led to the discovery of (S)-2-{[3′-(4-chloro-2,5-dimethylphenylsulfonylamino)-3,5-dimethylbiphenyl-4-carbonyl]-methylamino}-4-dimethylaminobutyric acid methyl ester **14**. Methyl ester prodrug **14** is hydrolyzed in vivo to the corresponding carboxylic acid **15**, a potent and selective S1P$_1$ antagonist. Oral administration of the prodrug **14** induces sustained peripheral blood lymphocyte reduction in rats. In a rat cardiac transplantation model coadministration of a nonefficacious dose of prodrug **14** with a nonefficacious dose of sotrastaurin (**19**), a protein kinase C inhibitor, or everolimus (**20**), an mTOR inhibitor, effectively prolonged the survival time of rat cardiac allografts. This demonstrates that clinically useful immunomodulation mediated by the S1P$_1$ receptor can be achieved with an S1P$_1$ antagonist generated in vivo after oral administration of its prodrug.

■ INTRODUCTION

Sphingosine 1-phosphate (S1P), a metabolite of sphingomyelin, is a bioactive sphingolipid and interacts with five S1P receptors (S1P$_1$–S1P$_5$), a family of cell-surface G-protein-coupled receptors.[1] The S1P receptors are expressed in many tissues, and S1P and the S1P receptors are involved in important regulatory functions both in normal physiology and disease processes such as apoptosis, cell migration, endothelial barrier function, vascular tone, and neural cell communication.[2]

The S1P$_1$ receptor is expressed in most immune cells, including B and T cells, and plays a key role in controlling the trafficking of lymphocytes from the lymphoid organs and the thymus into blood.[3] Modulation of the S1P$_1$ receptor with an agonist and with an antagonist causes inhibition of lymphocyte egress from lymph nodes and thymus, leading to immunomodulation.[4−7] A broad range of chemical probes have been identified demonstrating that S1P$_1$ agonists are efficacious in various animal models for transplantation and autoimmune diseases including experimental autoimmune encephalomyelitis, adjuvant- or collagen-induced arthritis, and lupus nephritis.[8−13] Furthermore, the S1P$_1$ agonist 2-amino-2-(4-octylphenethyl)-propane-1,3-diol (fingolimod, FTY720) is approved for the treatment of relapsing forms of multiple sclerosis.[14] To the best of our knowledge, only recently potent S1P$_1$ antagonists with demonstrated oral in vivo activity in animal models were described in the literature (Figure 1). In a mouse collagen-induced arthritis model **1** (TASP0277308) significantly suppressed the development of arthritis at a dose of 100 mg/kg po,
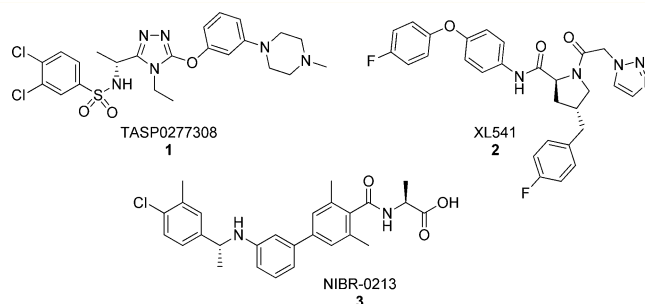

Figure 1. Structures of S1P$_1$ antagonists with oral in vivo activity.

b.i.d.[15] At this dose **1** also effectively inhibited tumor angiogenesis in mice.[16] In a MDA-MB-231T mouse xenograft model **2** (XL541) significantly inhibited tumor growth when given orally for 14 days at 100 mg/kg po, q.d.[17] Therapeutic treatment (26 days, 30 and 60 mg/kg po, b.i.d.) of **3** (NIBR-0213) in a mouse experimental autoimmune encephalomyelitis model resulted in gradual reduction in disease scores.[18]

There is a high need for S1P$_1$ antagonists preferably with high subtype selectivity to better understand their therapeutic potential and potential mechanism-based liabilities. In particular, we aimed for a selective S1P$_1$ antagonist with long lasting, reversible lymphocyte sequestration from circulation at a

reasonable oral dose to explore efficacy in a rat heart transplantation model.

■ RESULTS AND DISCUSSION

At the onset of this work, **4** was available as chemical starting point, which resulted from our efforts to find a potent and selective $S1P_1$ antagonist (Figure 2).[7] Compound **4** is highly
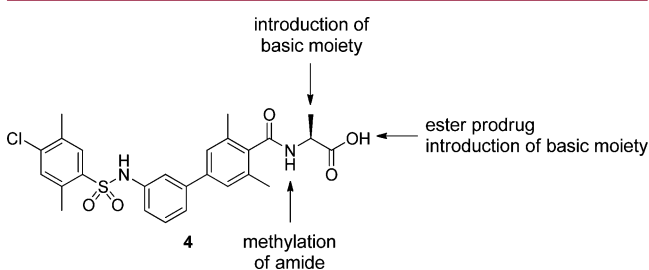

Figure 2. Structure of **4** and strategies for optimization.

potent in the $GTP\gamma^{35}S$ binding assay (Table 1) and efficiently reduces peripheral lymphocyte counts in Lewis rats, both after subcutaneous and after oral administration. However, the duration of action was limited. A high oral dose (100 mg/kg) was necessary to significantly reduce at 8 h the number of lymphocytes in blood (20% of the control values), and control lymphocyte counts were reestablished within 24 h (Table 2). It was likely that the poor permeability (log P_e (permeability coefficient defined by PAMPA) of −8.3 at pH 6.8) of **4** was leading to absorption limited blood levels, thus contributing to the short duration of action in the peripheral blood lymphocyte (PBL) reduction assay. Our goal was to achieve sustained systemic exposure to maintain full PBL reduction over 24 h after a single dose of 30 mg/kg po, achieving the same effect as with a selective $S1P_1$ agonist.[8]

We envisioned two optimization strategies to modify the oral exposure of the scaffold. This could be achieved by reducing the polar surface area (PSA) of **4**, either by alkylating the amide or by masking the carboxylic acid as an ester prodrug and by modulating the solubility by introducing basic moieties (Figure 2).[19−22] To broadly explore the potential of such a prodrug approach, we selected the corresponding carboxylic acids based on potency in the $GTP\gamma^{35}S$ assay and evaluated all compounds in the PBL reduction assay. For all carboxylic acids the $GTP\gamma^{35}S$ values are reported in Table 1, and the in vivo efficacy results of the corresponding prodrug esters in the PBL reduction assay are reported in Table 2.

First, we explored the effect of amide alkylation. Methylamide of **4**, **5** was highly potent in the $GTP\gamma^{35}S$ (6.1 ± 1.02 nM) assay, and oral administration of **5** (100 mg/kg) induced reduction of lymphocytes to 19% versus control for 12 h. The increased duration of action in the PBL reduction assay was likely due to better absorption (log P_e = −7.7 at pH 6.8). Next, we investigated the effect of masking the carboxylic acid as an ester, which could act as a prodrug and liberate the carboxylic acid by in vivo hydrolysis. Methyl ester of **4**, **6** is only weakly active in the $GTP\gamma^{35}S$ assay (6733 ± 1105 nM). However, oral application of **6** (100 mg/kg) reduced the lymphocyte counts to 24% versus control up to 14 h. This in vivo effect can only be rationalized by the presence of the highly potent **4** in blood which resulted from the hydrolysis of methyl ester **6**. This was confirmed by analysis of the blood samples.
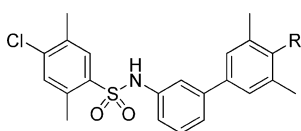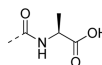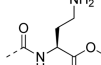
Table 1. Activity of Carboxylic Acids in the $GTP\gamma^{35}S$ Binding Assay
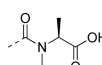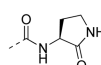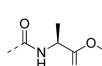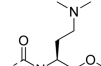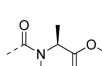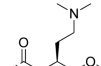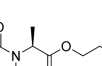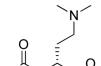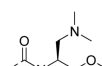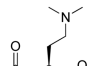
Cpd	R	$GTP\gamma^{35}S$ $IC_{50}{}^{a}$ (nM)
4		2.6 ± 0.06
5		6.1 ± 1.02
28		8.4 ± 1.8
11		2.1 ± 0.71
32		12 ± 0.35
15		3.4 ± 0.35
17		20 ± 1.7

[a]IC_{50} values are reported as the mean of at least three separate determinations ± SEM.

Finally, amide methylation and methyl ester were combined to provide **7**. We expected higher absorption for **7** versus **6** and a longer duration of action in the PBL reduction assay. Disappointingly, the duration of action was in the same range as for **6** after oral administration of the same dose. We reasoned that the low solubility of compound **7** (<0.004 mM at pH 6.8) became the absorption limiting factor. As a result, we concentrated our efforts on improving the solubility by introducing solubilizing groups in the pro-moiety as well as in the parent drug. First, introduction of a dimethylamino group into the pro-moiety provided dimethylaminoethyl ester **8**. This led to a significant longer duration of action. After an oral dose of only 30 mg/kg lymphocytes were reduced to 25% (14 h) and 49% (24 h) compared to control values, which was likely because of better solubility (0.015 mM at pH 6.8). Compounds with a basic group in the parent drug were then evaluated. Administration of compound **9**, with a dimethylaminomethyl side chain, induced only a reduction to 37% of circulating lymphocytes at 14 h versus control despite a high dose of 100 mg/kg po. Since **9** has high permeability (log P_e =

Table 2. Administered Dose in PBL Reduction Assay and Percent Remaining Lymphocytes versus Control at Given Time Points

Cpd	R	Dose[a]	PBL count (%) at given time[b]	Cpd	R	Dose[a]	PBL count (%) at given time[b]
4	(structure)	100	20 (8 h)	10	(structure)	100	76 (14 h)
5	(structure)	100	19 (12 h)	12	(structure)	100	no PBL reduction
6	(structure)	100	24 (14 h)	13	(structure)	100	15 (14 h) 24 (24 h)
7	(structure)	100	21 (14 h)	14	(structure)	30	21 (14 h) 22 (24 h)
8	(structure)	30	25 (14 h) 49 (24 h)	16	(structure)	30	67 (14 h)
9	(structure)	100	37 (14 h)	18	(structure)	30	28 (14 h) 48 (24 h)

[a]Dose: mg/kg po. [b]Remaining percent of circulating lymphocytes in blood versus control.

−4.9 at pH 6.8), the absorption is likely limited by the low solubility (<0.004 mM at pH 6.8). Further side chain variations were probed. Analogue **10**, with an aminoethyl side chain, displayed only marginal PBL reduction 14 h after a 100 mg/kg po dose, although the corresponding carboxylic acid **11** was highly potent in the GTPγ[35]S assay (2.1 ± 0.71 nM). We attributed the lack of in vivo activity of **10** to the low permeability (log P_e = −6.8 at pH 6.8) of the primary amine derivative. In addition, we had observed that the corresponding lactam **12** was formed readily from **10** if the pH was not acidic. The lactam **12** was only weakly active in the GTPγ[35]S assay (163 ± 42 nM) and did not lead to a reduction of lymphocyte counts after an oral dose of 100 mg/kg. To improve permeability and prevent potential in vivo lactam formation, the amino group of **10** was dimethylated. Compound **13** displayed improved permeability (log P_e = −5.1 at pH 6.8), and a dose of 100 mg/kg po induced full PBL reduction for 24 h (24% lymphocytes remaining versus control values). Knowing that amide methylation had a beneficial effect on the duration of action, we investigated the combination with a basic moiety in the side chain. The resulting analogue **14** had high permeability (log P_e = −4.6 at pH 6.8), and the corresponding carboxylic acid **15** was highly potent in the GTPγ[35]S assay (3.4 ± 0.35 nM). Administration of compound **14** (30 mg/kg po)

promoted a persistent reduction of lymphocyte counts for 24 h. The enantiomer of **14**, **16** was also investigated. Only a modest reduction of lymphocytes versus control values (67% at 14 h) was observed after oral dosing of 30 mg/kg. This is not unexpected given the reduced potency of the corresponding carboxylic acid **17**. Last, the ethyl ester of **15**, **18**, was explored. The in vivo effect of ethyl ester **18** was somewhat reduced compared to methyl ester **14** showing only 28% (14 h) and 48% (24 h) lymphocyte reduction in the PBL reduction assay after a dose of 30 mg/kg po. Various factors can lead to this reduced in vivo effect, such as permeability (log P_e = −5.0 at pH 6.8), solubility (<0.004 mM at pH 6.8), and in vivo hydrolysis rate.

In summary, we achieved our goal to significantly improve the duration of action in the PBL reduction assay after oral administration. Starting from **4**, we identified **14**, a prodrug with sustained oral efficacy by amide methylation, masking the carboxylic acid as a methyl ester and introducing a basic moiety in the side chain.

Characterization of the Prodrug 14 and the Active Moiety 15. Before starting further in vivo studies with **14**, we characterized the **14/15** prodrug/drug pair in more detail. Schild plot analysis indicated that **15** is a competitive S1P$_1$ antagonist with a calculated K_D of 0.67 ± 0.2 nM (Figure S1,

Table 3. S1P Receptor Subtype Selectivity of Carboxylic Acid 15 in the GTPγ^{35}S Binding Assays

	hS1P$_1$	hS1P$_2$	hS1P$_3$	hS1P$_4$	hS1P$_5$
IC$_{50}$,^{a} (nM)	3.4 ± 0.35	>10000	802 ± 76	>10000	978 ± 59
EC$_{50}$,^{a} (nM)	>10000	>10000	>10000	1195 ± 158	>10000

^{a}Antagonistic (IC$_{50}$) and agonistic (EC$_{50}$) activities for the subtype receptors are reported. IC$_{50}$ and EC$_{50}$ values are reported as the mean of at least three separate determinations ± SEM.

Supporting Information). Compound **15** is a highly selective S1P$_1$ antagonist. No activity was measured on the S1P$_2$ receptor subtype (Table 3). The selectivity of **15** against the S1P$_3$ and S1P$_5$ receptor subtypes is more than 200-fold, where a weak antagonistic activity was measured in the GTPγ^{35}S binding assays. No antagonistic activity was measured on the S1P$_4$ receptor subtype; however, **15** is a weak human S1P$_4$ agonist. Compound **15** was also tested for selectivity against a diverse panel of receptors, and up to 10 μM no appreciable binding affinity was observed.

Although S1P$_1$ agonists like fingolimod and the S1P$_1$ antagonist **15** have similar effects on PBL counts, they act through different mechanisms. Agonists lead to S1P$_1$-dependent intracellular signaling followed by receptor internalization and degradation.[14,23,24] The S1P$_1$ signaling is responsible for the activation of the GIRK channel, which has been associated with heart rate reduction in humans.[25,26] In rodents S1P$_3$ is responsible for heart rate changes.[27] It has been shown that the selective S1P$_1$ antagonist **3** does not lead to S1P$_1$-dependent signaling and does not induce S1P$_1$ receptor internalization.[18] In addition, **3** lacks GIRK activation and blocks agonist induced receptor internalization. S1P$_1$ antagonists, devoid of GIRK channel activity, are not expected to cause bradycardia in humans. S1P$_1$ antagonist **15** does not induce S1P$_1$-dependent signaling and does not lead to GIRK activation.

Ideally, the prodrug **14** should be chemically stable under the formulation conditions and during oral administration. Compound **14** should undergo enzymatic cleavage in vivo during the absorption and distribution processes to release the active species **15** into the circulation. For the determination of the blood levels of both species, further ester cleavage after blood sampling has to be stopped. To investigate potential contributions of nonenzymatic cleavage through chemical hydrolysis, we probed the chemical stability of **14** at different pH by UPLC. At pH 1 and 5 methyl ester **14** was stable for >53 h and none of the active moiety **15** was detected (Figure 3, data
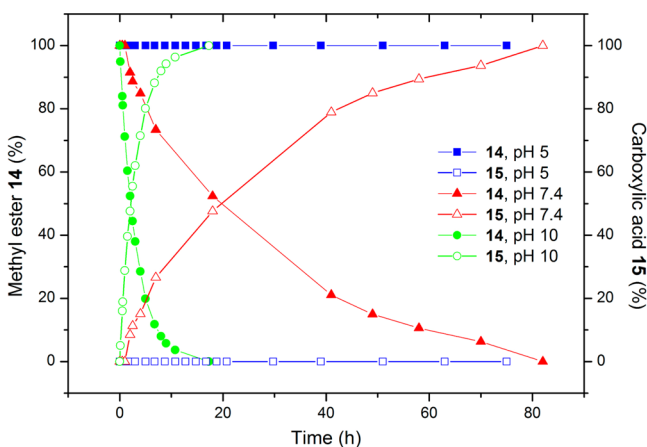
at pH 1 not shown). However, at pH 7.4 hydrolysis to the carboxylic acid was observed. Already after 2 h 9% of **15** was present and the amount of hydrolyzed species continuously increased to 48% (18 h) and 85% (49 h). After 82 h no more methyl ester could be detected by UPLC. At pH 10 hydrolysis of methyl ester **14** was significantly faster than at pH 7.4 with only 52% ester remaining after 2 h. After 17 h no more methyl ester **14** was detected. These data pointed out the importance of carefully adjusting the pH of the formulations used for in vivo experiments. All samples with methyl ester **14** were freshly prepared before dosing by dissolving the compound in a mixture of PEG200 and water and adjusting the pH to 5 with aqueous HCl (0.1 M). For the determination of blood levels of both the prodrug and the active moiety at different time points during in vivo experiments it was necessary to prevent further hydrolysis of the prodrug after sampling. This was ensured by stabilizing the blood by sampling immediately in EDTA coated Eppendorf vials containing aqueous citric acid (2 M). By use of this procedure, the pH of the blood samples was adjusted to 4.4 and further chemical hydrolysis was inhibited. Seemingly, this procedure also stopped further enzymatic hydrolysis, since the same results were obtained when esterase inhibitors were added. Furthermore, storage of the samples did not change the blood levels.

After isolation and purification of **14** several minor signals were observed in the NMR as well as an additional peak (peak A) in the UPLC (Figure 4). According to UPLC the ratio of peak A:B was 7:93. We anticipated that because of the amide methylation, the rotation around the amide bond might be hindered and therefore the minor peak A could arise from the (Z) amide conformer of **14**. This hypothesis was supported by the fact that the same mass was observed for peak A and peak B. If peak A and peak B were indeed amide conformers, a sample enriched with peak A should equilibrate to provide again a peak ratio A:B of 7:93. It is possible to separate peak A and peak B on silica, and column chromatography of **14** provided a fraction with a peak ratio A:B of 55:45. This sample was monitored by UPLC over time. The amount of peak A decreased over time while the amount of peak B increased (Figure 5). After 24 h a ratio of 14:86 was observed, and after 6 days the equilibrium ratio of 7:93 was reached, matching the initially determined ratio for **14** after isolation. For additional confirmation and for unambiguous assignment of the amide conformers we also investigated the equilibration by ^{1}H NMR. We were able to separate peak A and peak B by preparative HPLC. Removal of the solvent at low temperature and storage of the isolated sample on dry ice afforded a sample with a ratio A:B of 65:35 as determined by ^{1}H NMR (Figure 6). The proton in the position α to the ester (H-32) and the methyl group of the ester (H-40) were monitored (Figure 7). The signals of conformer A decreased over time, and the signals of conformer B increased. After 14.4 h the ratio of A:B was 14:86, and after 6 days equilibrium was reached with A:B of 7:93. Furthermore, the conformers A and B were characterized by ^{1}H and ^{13}C NMR. The ^{13}C shift differences between the two

Figure 3. Hydrolysis of methyl ester **14** to carboxylic acid **15** at different pH.
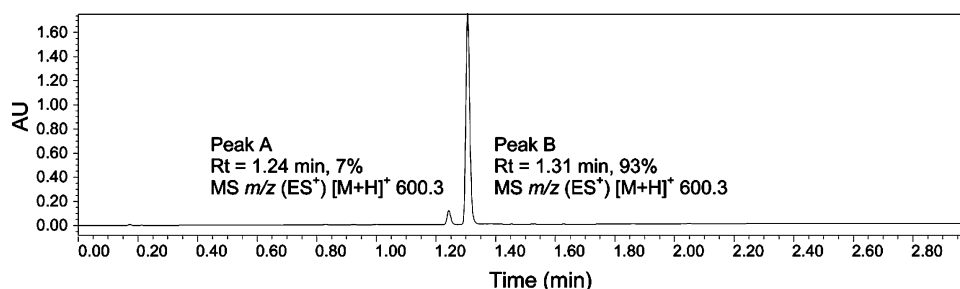
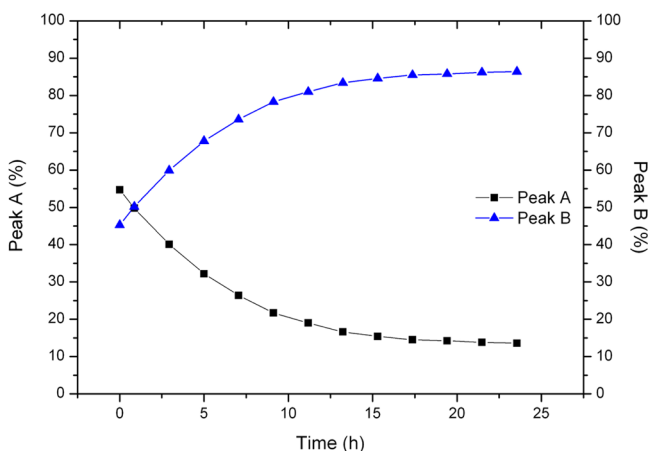**Figure 4.** UPLC of **14** at equilibrium.

Figure 5. Equilibration of methyl ester **14** amide conformers A and B monitored by UPLC.

conformers are 4.7 ppm for C-31 and 4.0 ppm for C-32 (Figure 7). These differences are comparable with those observed in (Z) and (E) amide conformers.[28,29] The ^{1}H NMR shifts of the N-methyl groups H-31 show a difference of 0.32 ppm, while the expected ^{1}H shift difference of N-methyl groups between (Z) and (E) isomers is 0.12 ppm. In conformer B the N-methyl group H-31 is high field shifted. In contrast, in conformer A the α-proton H-32 and H-35, H-36, H-38, and H-41 are high field shifted. These high field shifts can be explained by the shielding effect by the inner ring current of the aromatic system attached to the amide. The data suggest that in conformer A the complete amino acid side chain including H-32 is placed above the aromatic ring and the methyl ester group points to the other direction, leading to the conclusion that conformer A corresponds to the (Z) amide. In conformer B only the methyl group H-31 is affected by the high field shift and the amino acid side chain has normal shifts, which is in agreement with the (E) amide. The chemical shift differences of protons and carbons of the amino acid residue in both conformers allow the unambiguous assignment of the amide conformers, conformer A corresponding to the (Z) amide and conformer B to the (E) amide of **14**. In summary, both UPLC and ^{1}H NMR analyses confirmed the presence of two amide conformers in **14** with the (E) conformer being the major at equilibrium.

In Vivo Evaluation of 14. Oral administration of **14** (30 mg/kg po) induced a rapid decrease in the number of
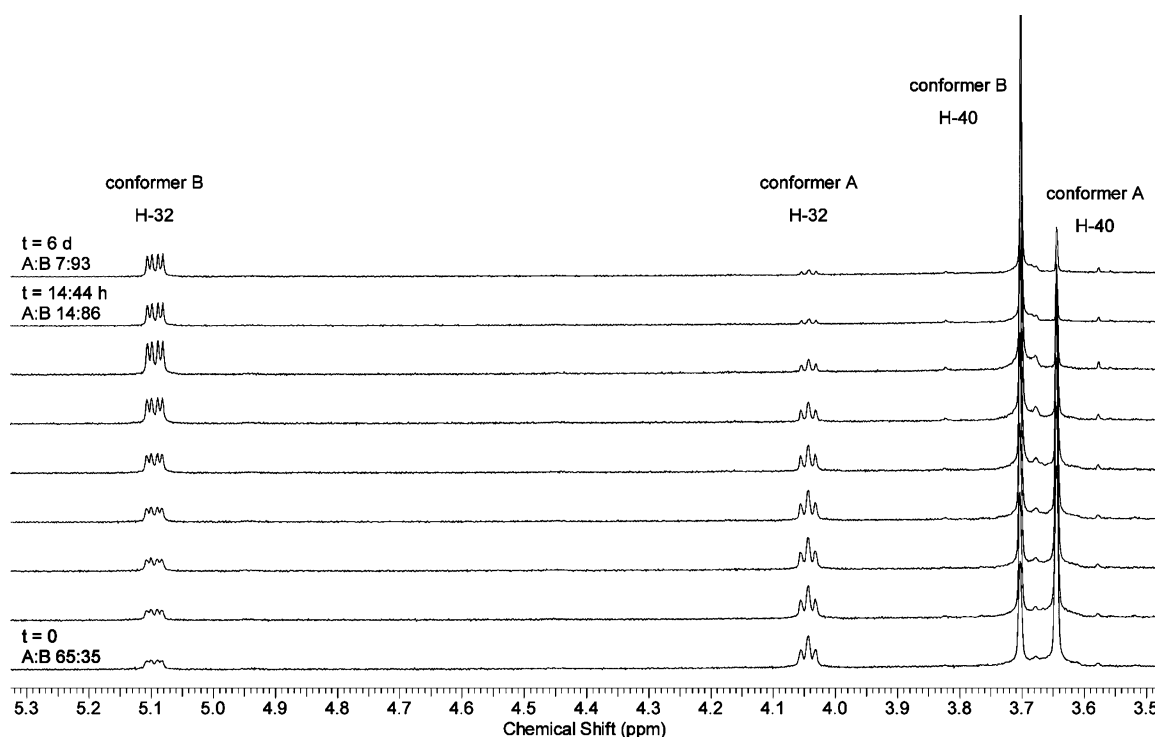

Figure 6. Equilibration of methyl ester **14** amide conformers A and B monitored by ^{1}H NMR.

Conformer A		Δppm	Conformer B	
δ ^{1}H-31	3.02 ppm	0.32	δ ^{1}H-31	2.7 ppm^a
δ ^{13}C-31	28.8 ppm	4.7	δ ^{13}C-31	33.5 ppm
δ ^{1}H-32	4.04 ppm^a	1.04	δ ^{1}H-32	5.09 ppm
δ ^{13}C-32	59 ppm	4.0	δ ^{13}C-32	55 ppm
δ ^{1}H-35	1.79, 2.04 ppm		δ ^{1}H-35	1.98, 2.16 ppm
δ ^{1}H-36	2.16 ppm		δ ^{1}H-36	2.29, 2.39 ppm
δ ^{1}H-38	2.00 ppm		δ ^{1}H-38	2.19 ppm
δ ^{1}H-41	2.00 ppm		δ ^{1}H-41	2.19 ppm

^{a}Shielding by inner ring current

(Z) conformer   **(E) conformer**
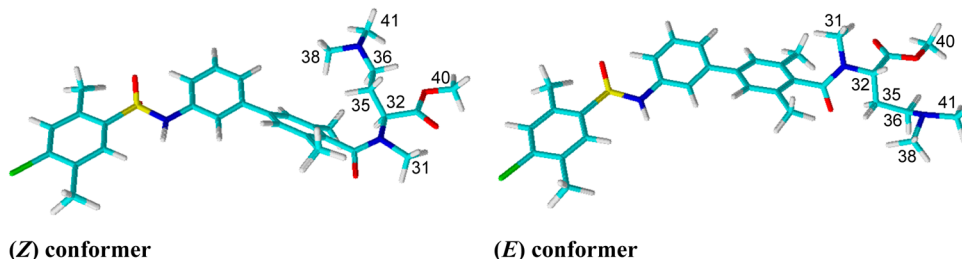
Figure 7. Assignment of amide conformers by ^{1}H and ^{13}C NMR.

peripheral lymphocytes in Lewis rats (Figure 8). Reduction of circulating lymphocytes was maintained for 24 h, and peripheral
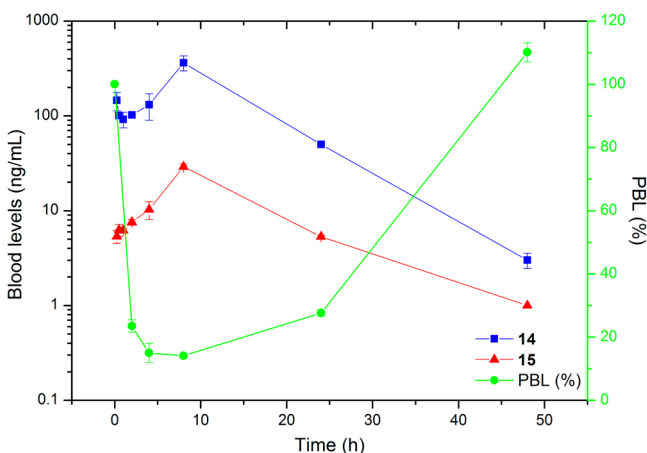

Figure 8. Lymphocyte counts and blood levels of **14** and **15** after administration of methyl ester **14** (30 mg/kg po). The baseline value of PBL (100%) corresponds to 7745 lymphocytes per microliter.

lymphocyte counts returned to pretreatment levels 48 h after compound administration. Analysis of the blood levels revealed that methyl ester **14** and the corresponding carboxylic acid **15** were present over 24 h. The methyl ester **14** itself is not an S1P$_1$ antagonist. Compound **14** is hydrolyzed in vivo to the potent S1P$_1$ antagonist **15** which is responsible for the in vivo effect. For the prodrug **14** a two-phase absorption was observed leading to an early peak after 0.25 h (146 ± 32 ng/mL) and a maximum concentration after 8 h (364 ± 65 ng/mL). After 24 h low levels of **14** could still be detected in the blood (50 ± 4 ng/mL). For the active moiety **15** the levels were low over 24 h. The maximum concentration was detected at 8 h (29 ± 2 ng/mL), and after 24 h only very low levels of **15** were measured (5 ± 0 ng/mL). Despite the low levels of the active species, lymphocyte sequestration was maintained for 24 h after

a single dose, suggesting that the methyl ester **14** acted as a reservoir, continuously generating active species **15**.

Having shown that a single oral dose of **14** leads to lymphocyte sequestration over 24 h, repeated dosing was investigated to probe the potential of the compound in a chronic setting. Prodrug **14** was dosed daily (30 mg/kg po) over 5 days, and lymphocytes were measured once a day before administration of the next dose. Circulating lymphocytes were reduced to around 20% of control values over the whole experiment, confirming the immunomodulation after repeated application (data not shown). It has been shown that S1P$_1$ antagonists induce capillary leakage in rodent lungs.[15,30] We investigated the acute and chronic effects of **14** in an Evans blue dye (EBD) lung leakage model.[30] Compound **14** was applied b.i.d. (30 mg/kg po) to Lewis rats, and the EBD increase versus control was measured at 6 h (after one dose), 24 h (two doses), and 96 h (eight doses). At 6 h a (3.0 ± 0.4)-fold EBD increase was measured, at 24 h a (2.4 ± 0.4)-fold increase, and at 96 h a (2.2 ± 0.3)-fold increase (Figure 9). Fluid was found in the thorax at 6 h (1.00 ± 0.22 mL) and 24 h (2.00 ± 0.57 mL). However, after 96 h no fluid could be detected in the thorax. These data suggest that the pulmonary leakage is a transient effect that decreases after multiple dosing. The physiological consequences of such an effect are not yet known. Further safety investigations are necessary to understand the long-term effect of S1P$_1$ antagonists on lung permeability.

These data encouraged us to test the prodrug **14** in a rat heart transplantation model to investigate if the observed immunomodulation translates into prolonged allograft survival. Methyl ester **14** was tested in the stringent DA (Dark Agouti) to Lewis rat heterotopic vascular heart allotransplantation model in combination with a nonefficacious dose of 3-(1H-indol-3-yl)-4-[2-(4-methylpiperazin-1-yl)quinazolin-4-yl]-pyrrole-2,5-dione (sotrastaurin, **19**),[31] a protein kinase C inhibitor, or everolimus (**20**),[32] an mTOR inhibitor. In vehicle treated recipient rats, DA grafts were acutely rejected on day 6 (Table 4). In recipient rats treated with **14** alone at 30 mg/kg po, b.i.d., grafts were rejected within 10 days with a median graft survival time (MST) of 8 days, and severe acute rejection
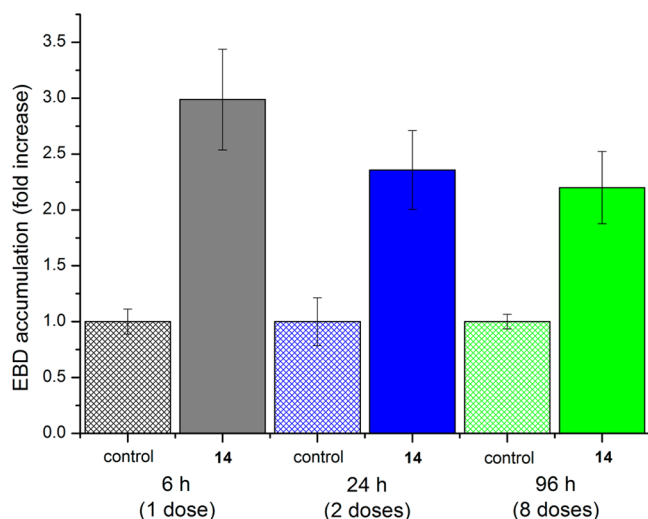
Figure 9. EBD accumulation in rat lungs after single and repeated dosing of **14** (30 mg/kg po b.i.d.).

was confirmed by histology. At this dose **14** did not prevent graft rejection, but it was capable of strongly mediating sustained lymphocyte counts. In recipients treated with **19** (10 mg/kg po, b.i.d.) or with **20** (0.3 mg/kg po, q.d.) all grafts were rejected at day 7, with severe acute rejection confirmed by histology. In contrast, combination therapy of **14** (30 mg/kg po, b.i.d.) with either **19** (10 mg/kg po, b.i.d.) or **20** (0.3 mg/kg po, q.d.) showed a synergistic effect leading to pronounced prolongation of heart allograft survival. For both combination treatments all grafts remained functional until the predetermined termination point of 50 days. Histological analysis of the grafts confirmed that acute rejection was only mild to moderate in the group co-treated with **19**, whereas it was absent to mild in the group co-treated with **20**. Cardiac allograft vasculopathy developed in all grafts co-treated with **19** (mild to severe) but in none of the grafts co-treated with **20**. Multifocal interstitial fibrosis was also observed in three grafts co-treated with **19** and in only one graft co-treated with **20**. Despite the acute vascular leakage in the EBD model, the treatment was well tolerated and a normal increase of body weight was observed. Besides mild perivascular edema, there were no histopathological findings in the lung in both co-treatment groups. The number of peripheral lymphocytes was measured once a week, always before treatment. Lymphocytes were reduced to 12−29% versus control in the group co-treated with **19** and to 9−22% versus control in the co-treatment group with **20** over the whole treatment period of 50 days. PK analysis confirmed in vivo hydrolysis of the ester **14** to the active moiety **15** and

revealed no drug−drug interactions. Combination therapy did not affect the blood levels of both immunomodulating agents.

These results are comparable to treatment with $S1P_1$ agonists in the same model. Fingolimod (0.1 mg/kg po, q.d.) co-treatment with **19** (10 mg/kg po, b.i.d.) or **20** (0.3 mg/kg po, q.d.) led to a MST of >68.5 or 38 days, respectively.[33,34] With the selective $S1P_1$ agonist (3-(((2-(2-(trifluoromethyl)-[1,1′-biphenyl]-4-yl)benzo[b]thiophen-5-yl)methyl)amino)-propanoic acid) (10 mg/kg po, q.d.) in combination with **20** (0.3 mg/kg po, q.d.) all grafts reached the termination point of 26 days, showing moderate acute cellular rejection.[8] Thus, oral combination therapy of the $S1P_1$ antagonist prodrug **14** with **19** or with **20** significantly prolonged cardiac allograft survival. It was shown that the selective $S1P_1$ antagonist **15**, generated in vivo after oral administration of its methyl ester prodrug **14**, mediates potent immunomodulation leading to increased graft protection in a transplantation model.

CHEMISTRY

Intermediate **21** was obtained by Suzuki coupling of 4-bromo-2,6-dimethylbenzoic acid (**22**) with 3-aminophenylboronic acid to afford **23** followed by reaction with 4-chloro-2,5-dimethylphenylsulfonyl chloride (Scheme 1). The amide coupling reaction to introduce the different amino acid head groups was carried out by formation of the acid chloride of **21** followed by addition of the corresponding amines. For the synthesis of **6**, (S)-2-aminopropionic acid methyl ester hydrochloride (**24**) was used in the amide coupling reaction (Scheme 2). Compound **7** was obtained by using (S)-2-methylaminopropionic acid methyl ester hydrochloride (**25**) for the coupling. Ester hydrolysis of **7** provided **5**. Subsequent esterification with 2-dimethylaminoethanol led to **8**. Compound **9** was obtained from intermediate **21** and (S)-2-methylamino-3-hydroxypropanoic acid methyl ester hydrochloride (**26**) and a subsequent conversion of the alcohol **27** to the tertiary amine with (cyanomethyl)-trimethylphosphonium iodide and dimethylamine hydrochloride.[35] Ester hydrolysis generated **28**. Amide coupling of (S)-2-amino-4-(($tert$-butoxycarbonyl)amino)butanoic acid methyl ester hydrochloride (**29**) with compound **21** provided the Boc protected intermediate **30** which was deprotected to give **10** (Scheme 3). To obtain the carboxylic acid **11**, intermediate **30** was first treated with aqueous base to provide the carboxylic acid **31** followed by Boc cleavage with HCl in dioxane. The lactam derivative **12** was obtained by deprotection of **30** with TFA followed by cyclization in refluxing toluene. The amino group of **10** was dialkylated by reductive amination with formaldehyde to yield **13**. Hydrolysis of the ester provided **32**. Reductive amination of **29** with benzaldehyde followed by an in

Table 4. Effect of Treatment of Oral 14 Alone and When Combined with Oral 19 or 20 on Survival of Rat Heart Allografts

treatment	dose (mg/kg po, b.i.d.)	dose (mg/kg po, q.d.)	graft survival (days)	median survival time (MST) (days)	acute cellular rejection scores[a]
control	0		6, 6, 6, 6	6	3R%, 3R%, 3R%, 3R%
14	30		8, 8, 10, 8	8	3R, 3R, 3R, 3R
19	10		7, 7, 7, 7	7	3R, 3R, 3R, 3R
20		0.3	7, 7, 7, 7, 7	7	3R, 3R, 3R, 3R, 3R
14 + 19	30 + 10		>50, >50, >50, >50	>50	2R[1#−3#$], 1R[1#,$], 2R[1#,$], 1R[1#−3#]
14 + 20	30	0.3	>50, >50, >50, >50	>50	0, 0, 1R, 1R$

[a]Acute cellular rejection score: 0 = no rejection, 1R = mild rejection, 2R = moderate rejection, 3R = severe rejection, 1# = mild cardiac allograft vasculopathy, 2# = moderate cardiac allograft vasculopathy, 3# = severe cardiac allograft vasculopathy, $ = multifocal interstitial fibrosis, % = diffuse necrosis.

Scheme 1. Synthesis of Intermediate 21[a]
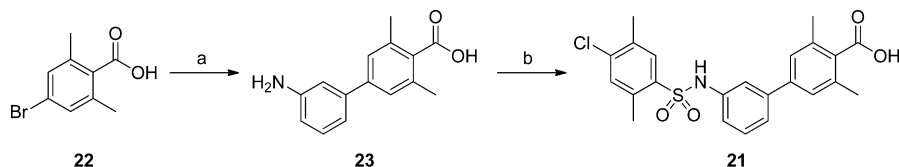
[a]Reagents: (a) 3-aminophenylboronic acid, aqueous NaHCO$_3$, Pd(PPh$_3$)$_4$, DME; (b) 4-chloro-2,5-dimethylphenylsulfonyl chloride, pyridine, dichloromethane.

Scheme 2. Synthesis of Prodrugs 6−9 and Carboxylic Acid Derivatives 5 and 28[a]
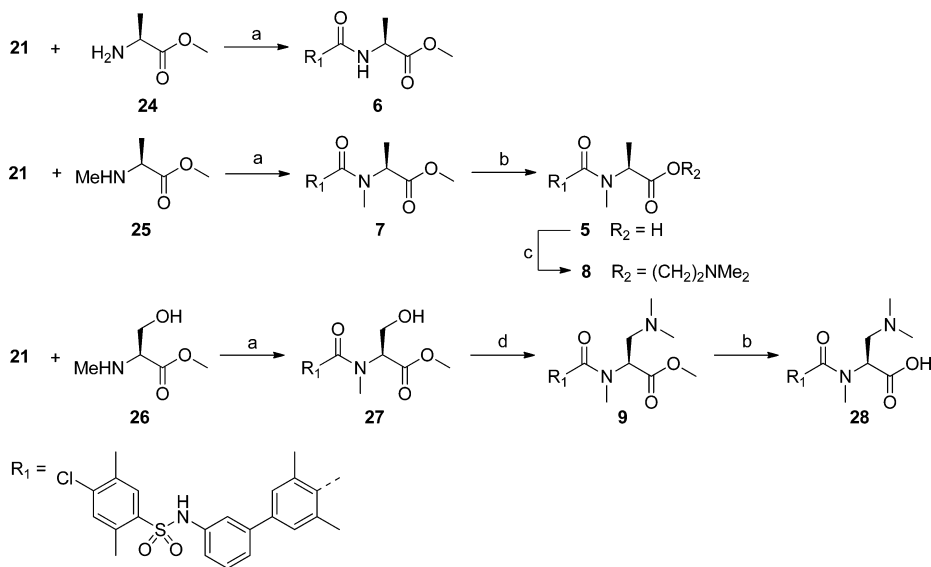
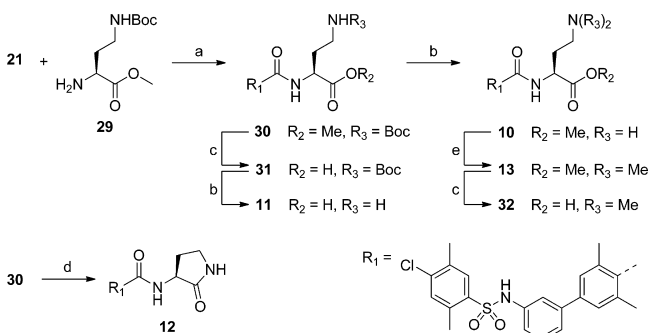[a]Reagents: (a) (i) SOCl$_2$, dichloromethane, (ii) DIPEA, THF; (b) aqueous LiOH, THF; (c) HOCH$_2$CH$_2$NMe$_2$, Boc$_2$O, DMAP, THF; (d) Me$_2$N·HCl, DIPEA, (Me$_3$PCH$_2$CN)I, propionitrile.

Scheme 3. Synthesis of Prodrugs 10 and 13, Lactam 12, and Carboxylic Acid Derivatives 11 and 32[a]

[a]Reagents: (a) (i) SOCl$_2$, dichloromethane, (ii) DIPEA, THF; (b) HCl, dioxane; (c) aqueous LiOH, THF; (d) (i) TFA, dichloromethane, (ii) toluene; (e) aqueous formaldehyde, NaCNBH$_3$, methanol.

Scheme 4. Synthesis of Building Blocks 34 and 38[a]
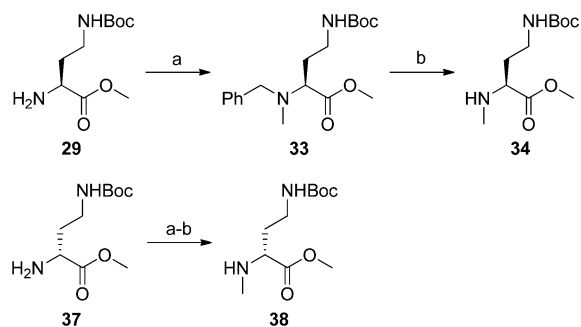
[a]Reagents: (a) (i) benzaldehyde, DIPEA, AcOH, NaCNBH$_3$, methanol, (ii) aqueous formaldehyde; (b) H$_2$, Pd(OH)$_2$, methanol.

situ second reductive amination with formaldehyde afforded intermediate **33** (Scheme 4). Debenzylation gave amine **34**, which was used as crude in the amide coupling with intermediate **21** to provide **35** (Scheme 5). Deprotection of the Boc group generated the amine **36**, which was converted to **14** by reductive amination. Hydrolysis of **14** generated carboxylic acid **15**. The enantiomer of **14**, **16** was obtained following the same sequence starting with (*R*)-2-amino-4-((*tert*-butoxycarbonyl)amino)butanoic acid methyl ester hydrochlor-

ide (**37**) (Scheme 4 and Scheme 5). Basic hydrolysis of **16** yielded the carboxylic acid **17**. Esterification of **15** with ethanol provided ethyl ester **18**.

■ CONCLUSIONS

A prodrug approach was successfully applied to modulate the duration of the pharmacodynamic effect of the selected scaffold for chronic efficacy studies in a rat heart transplantation model. A broad scaffold exploration by amide methylation, masking the carboxylic acid as an ester and introducing basic moieties, led to the identification of **14**.

Scheme 5. Synthesis of Prodrugs 14, 16, and 18 and Carboxylic Acid Derivatives 15 and 17[a]
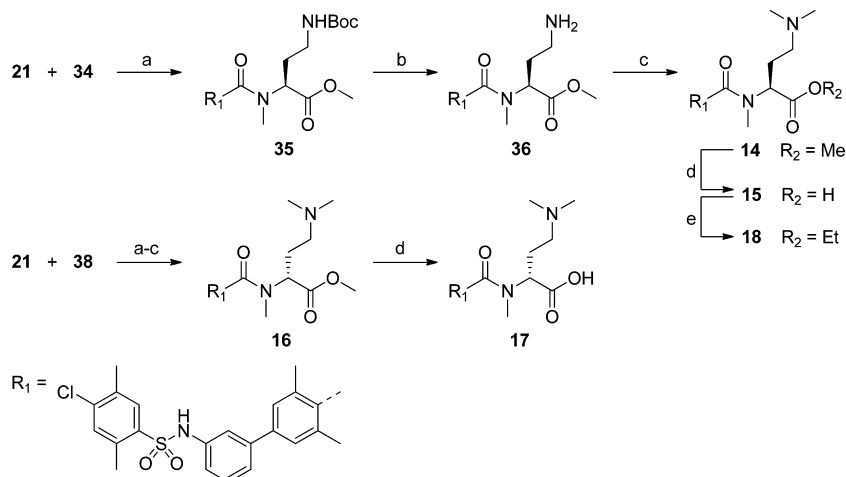
[a]Reagents: (a) (i) $SOCl_2$, dichloromethane, (ii) DIPEA, THF; (b) HCl, dichloromethane; (c) aqueous formaldehyde, AcOH, $NaBH(OAc)_3$, acetonitrile; (d) aqueous LiOH, THF; (e) EtOH, Et_3N, DMAP, propylphosphonic anhydride, THF.

Upon oral administration **14** was hydrolyzed in vivo to the corresponding carboxylic acid **15**, a highly potent and selective $S1P_1$ antagonist, which induced a long lasting, reversible reduction of circulating lymphocytes in the rat (full PBL reduction over 24 h after a single dose of 30 mg/kg po). In addition, oral administration of **14** in combination with a subtherapeutic dose of **19** or **20** in a stringent rat heart transplantation model effectively prolonged survival of cardiac allografts with excellent histology. These results suggest a synergy between complementary immunosuppressive modes of action. It is of note that **14** was very well tolerated during the entire observation period of up to 50 days after transplant. These data demonstrate that graft protection can be achieved by targeting the $S1P_1$ receptor with a selective antagonist, generated in vivo by hydrolysis of a prodrug, leading to similar efficacy as with $S1P_1$ agonists.

■ EXPERIMENTAL SECTION

GTPγ^{35}S. Membranes were prepared from CHO cell clones stably expressing a human $S1P_1$. The desired amount of membranes (1−5 μg/well) was diluted with assay buffer (50 mM HEPES, pH 7.4, 5 mM $MgCl_2$, 1 mM $CaCl_2$, 1% fatty acid-free BSA) containing 10 μM GDP, 25 μg/mL saponin, and 5 mg/mL WGA-SPA beads (Perkin-Elmer). Serial dilutions of compounds were incubated with 200 μL of membrane-WGA-SPA bead slurry for 15 min followed by the addition of the agonist S1P (4 nM final concentration). Then GTPγ^{35}S (0.2 nM final concentration) in assay buffer was added. After incubation at room temperature for 120 min under constant shaking the plates were centrifuged for 10 min at 1000g to pellet the membrane−SPA beads slurry. Then the plates were measured in a TOPcount NXT instrument (Perkin-Elmer). Eight different concentrations of compound were used to generate a concentration response curve (using two data points per concentration) and the corresponding IC_{50} using the curve-fitting tool of GraphPad Prism.

$S1P_2$, $S1P_3$, $S1P_4$, and $S1P_5$ dependent GTPγ^{35}S assays were carried out in a manner comparable to that of the $S1P_1$ GTPγ^{35}S assay using membranes from CHO cells stably expressing the S1P receptors.

Peripheral Blood Lymphocyte Reduction Assay. Male Lewis rats (Harlan CPB) were subjected to a single dose of either vehicle (control) or compound (all prepared fresh in a 30% PEG200/buffer solution) via oral administration. Longitudinal blood sampling (<200 μL) was performed under anesthesia (isoflurane 5% v/v; Forene, Abbott, Baar, Switzerland) by sublingual punctures at given time points (before compound administration (baseline) and 4, 8, 12, 24 h after drug application or 14, 18, 24, and 48 h after drug application). Whole blood was sampled in EDTA-coated Eppendorf tubes and subjected to hematology analysis. Lymphocyte counts were measured by an automated hematology analyzer (ADVIA 120, Bayer Diagnostics, Zurich, Switzerland). Individual changes in peripheral lymphocyte counts after vehicle or compound application were compared with the respective baseline value determined before start of treatment. Changes were then calculated as percent change compared to baseline values.

EBD Lung Leakage Model. Male Lewis rats (Harlan CPB) were treated orally (gavage), twice per day, with either vehicle (control) or **14** at 30 mg/kg (freshly prepared in a 30% PEG200/buffer solution). Leakage of plasma proteins in the lung was assessed using the standard Evans blue dye (EBD) leakage technique.[30] Briefly, EBD (Fluka) was administered intravenously (20 mg/2 mL NaCl/kg) under anesthesia at 5, 23, or 95 h after treatment. In each case, 1 h after EBD injection, the rats were bled under deep anesthesia by incision of the vena cava and the pulmonary vessels perfused via the right-ventricle with 10 mL of saline to remove blood and EBD from the vascular spaces. The lungs were collected en bloc and dried at 60 °C for 24 h. Dried lungs were weighed and immersed into 2 mL of formamide (Sigma) for 24 h at 37 °C in order to extract EBD from tissues. Each extract was then assessed by spectrophotometry at 620 and 740 nm to correct for contaminating heme pigments with the following formula: OD_{620} (EBD) = OD_{620} − [(1.426)(OD_{740}) + 0.030]. The EBD concentrations in lung extracts were finally estimated with the help of parallel EBD-standard curve.

Heterotopic Vascular Heart Transplantation DA-to-Lewis Rat Model. The heterotopic cardiac transplantation was performed as described previously.[36] The cooled and heparinized donor heart was removed following ligation of all vessels except the ascending aorta and the right pulmonary artery. These vessels were then anastomosed end-to-side to the recipient's abdominal aorta and inferior vena cava. After release of the clamps, the heart started to beat within less than 2 min. Graft function was assessed daily by palpation for ventricular contraction. Hearts in which ventricular motion had ceased were considered rejected, which was confirmed subsequently by histology. Body weight was monitored regularly.

Recipient rats received the following treatments: vehicle (po, b.i.d.), **14** (30 mg/kg po, b.i.d.), **19** (10 mg/kg po, b.i.d.), or **20** (0.3 mg/kg po, q.d.), all as monotherapy, or **14** (30 mg/kg po, b.i.d.) in combination with **19** (10 mg/kg po, b.i.d.) or **14** (30 mg/kg po, b.i.d.) in combination with **20** (0.3 mg/kg po, q.d.). Compound **14** was dissolved in PEG200, distilled water and acidified to pH 5 by addition of aqueous HCl (0.1 M). Compound **19** was mixed in D-glucose and dissolved in PEG400, distilled water, and aqueous HCl (0.1 M).

Microemulsion preconcentrate of **20** was diluted with distilled water. All solutions were freshly prepared daily. All treatments were performed by oral gavage using rat-feeding needles. Treatments with **14** and **20** were performed using a volume of 2 mL/kg, and treatments with **19** were performed using a volume of 3 mL/kg. In combination treatments the compounds were given one after the other, with **14** always applied first. Treatments started 3 days before transplantation. The experiments were terminated at rejection or at predefined termination points.

For histological examination, cardiac allografts were fixed in 10% buffered formalin, processed according to standard procedures, and embedded in paraffin. Tissue blocks were cut to 3 μm sections that underwent staining with hematoxylin and eosin (H&E) and trichrome. The degree of acute cardiac rejection was scored according to Stewart:[37] 0R, no rejection; 1R, mild; 2R, moderate; 3R, severe. In addition, the grade of cardiac allograft vasculopathy (CAV) was scored: 0, no CAV; 1, mild (<25% lumen occlusion); 2, moderate (26−50% occlusion); 3, severe (>50% occlusion).

NMR Study. The minor conformer A was separated from peak B by preparative HPLC, injecting a sample of the free base of **14**. The solvent was removed at low temperature, and the isolated sample was stored on dry ice. The NMR measurements were performed on a Bruker AV 600 spectrometer at 298 K, using a 1 mm TXI microliter probe. ^{1}H NMR spectra were measured with 32 scans, 4.233 s repetition time, 64 k time domains, and 2.733 s acquisition time, using a 30° pulse angle (zg30). The ROESY spectrum was obtained with 377 t_1 values (TD = 2 k, 16 scans), using a 200 ms ± 180° spinlock. The HSQC spectrum was run with 256 t_1 values (TD = 2 k, 8 scans) using adiabatic pulses for ^{13}C decoupling. The integration of the two conformers was done on H-32 (Figure 7), at 5.0−5.3 ppm for the major conformer B and at 3.9−4.2 ppm for the minor conformer A, after a manual baseline correction was applied between 3.8 and 5.4 ppm on each spectrum.

The NMR solution was prepared by dissolving 1 mg of compound (free base) in 18 μL of DMSO-d_6. An amount of ~9 μL was transferred into a capillary NMR tube. Nine measurements at different time points were acquired, where the decay of conformer A was observed. By use of the remaining solution, ^{1}H NMR, 2D-HSQC, and 2D-ROESY experiments were performed. [13]C shifts of the N-methyl group H-31 and the α-CH group H-32 of both conformers were taken from the HSQC spectrum for comparison. The protons of both conformers were assigned on the basis of the ROESY and the HSQC spectra.

Chemistry. All reagents and solvents were purchased from commercial suppliers and used without further purification or were prepared according to published procedures. All reactions were performed under inert conditions (argon) unless otherwise stated. ^{1}H NMR spectra were recorded on a Bruker 360 MHz or a Bruker 400 MHz NMR spectrometer. Chemical shifts are reported in parts per million (ppm) relative to an internal solvent reference. Significant peaks are tabulated in the order multiplicity (s, singlet; d, doublet; t, triplet; q, quartet; quintet; m, multiplet; br, broad; v, very), coupling constants, and number of protons. Analytical UPLC−MS was performed on a Waters Acquity UPLC instrument equipped with a PDA detector and a SQ mass spectrometer using a Waters Acquity UPLC BEH C18 2.1 mm × 30 mm, 1.7 μm column. Electrospray ionization (ESI) mass spectra were recorded on an Agilent 1100 series mass spectrometer. Mass spectrometry results are reported as the ratio of mass over charge. For all compounds containing amide conformers the percentage of each conformer was determined by analytical UPLC (Waters Acquity UPLC instrument equipped with a PDA detector and a Waters Acquity UPLC BEH C18, 2.1 mm × 50 mm, 1.7 μm column). Peak detection is reported as the maximum plot from 190 to 350 nm wavelength. The NMR data of both conformers are reported when the percentage of the minor is >5%; otherwise only the data of the major are given. The accurate mass analyses were performed by using electrospray ionization in positive mode after separation by LC. The elemental composition was derived from the averaged mass spectra acquired at a high resolution of about 30 000 on an LTQ Orbitrap XL mass spectrometer (Thermo Scientific). The high mass

accuracy below 1 ppm was obtained by using a lock mass. All final compounds were purified to ≥95% purity as assayed by analytical UPLC−MS (Waters Acquity UPLC instrument equipped with an PDA detector and a SQ mass spectrometer using a Waters Acquity UPLC BEH C18, 2.1 mm × 30 mm, 1.7 μm column) at a 1.0 mL/min flow rate with a gradient of 5−98% acetonitrile (containing 0.04% formic acid) in 0.05% aqueous formic acid (containing 3.75 mM ammonium acetate) for 9.4 min and a total run time of 10 min.

3′-(4-Chloro-2,5-dimethylphenylsulfonylamino)-3,5-dimethylbiphenyl-4-carboxylic Acid (21). To a mixture of 4-bromo-2,6-dimethylbenzoic acid (**22**) (1.66 g, 7.23 mmol) and tetrakis-(triphenylphosphine)palladium (25 mg, 0.022 mmol) in dimethoxyethane (200 mL) and aqueous sodium bicarbonate (10 wt %, 45 mL, 50.6 mmol) was added 3-aminophenylboronic acid (1.09 g, 7.95 mmol). The mixture was stirred at 100 °C for 1 h. When the mixture cooled, a brownish oily layer was formed which was carefully decanted. The solvents were evaporated. The residue was taken up in water and washed with diethyl ether. The pH of the aqueous layer was adjusted to about 4 with aqueous HCl (2 M), upon which a slightly sticky solid precipitated. The solid was filtered off, redissolved in ethyl acetate, and dried over sodium sulfate. Filtration and evaporation afforded 3′-amino-3,5-dimethylbiphenyl-4-carboxylic acid (**23**) (1.42 g, 84%) as a beige powder which was used without further purification for the next step. ^{1}H NMR (400 MHz, DMSO-d_6): δ (ppm) 7.25 (s, 2H), 7.09 (t, J = 7.8 Hz, 1H), 6.83 (br t, J = 1.9 Hz, 1H), 6.7 (v br d, J = 7.8 Hz, 1H), 6.57 (br ddd, J = 7.8, 1.9, 1.1 Hz, 1H), 3.35 (v br s, 2H), 2.33 (s, 6H). UPLC−MS m/z (ES⁻) (M − H)⁻ = 240.3. HRMS m/z (EI) (M + H)⁺ = 242.1173 (calcd for $C_{15}H_{16}NO_2$, 242.1181).

To a solution of **23** (1.34 g, 5.55 mmol) in pyridine (9 mL) was added dropwise a solution of 4-chloro-2,5-dimethylphenylsulfonyl chloride (1.33 g, 5.55 mmol) in dichloromethane (18 mL) over a period of 5 min. The resulting mixture was stirred at room temperature for 2 h. The mixture was diluted with dichloromethane and washed with aqueous HCl (2 M, 3×), water, and brine. The organic layer was dried over sodium sulfate, filtered, and concentrated to afford **21** (2.07 g, 83%) as an off-white solid. ^{1}H NMR (400 MHz, DMSO-d_6): δ (ppm) 13.22 (br s, 1H), 10.59 (s, 1H), 7.98 (s, 1H), 7.49 (s, 1H), 7.23−7.36 (m, 3H), 7.15 (s, 2H), 7.06 (br dt, J = 7.6, 1.8 Hz, 1H), 2.54 (s, 3H), 2.35 (s, 3H), 2.33 (s, 6H). UPLC−MS m/z (ES⁻) (M − H)⁻ = 442.3. HRMS m/z (EI) (M + H)⁺ = 444.1029 (calcd for $C_{23}H_{23}ClNO_4S$, 444.1036).

(S)-4-*tert*-Butoxycarbonylamino-2-methylaminobutyric Acid Methyl Ester (34). To a solution of (S)-2-amino-4-((*tert*-butoxycarbonyl)amino)butanoic acid methyl ester hydrochloride (**29**) (25.0 g, 93.0 mmol) in methanol (900 mL) was added DIPEA (17.8 mL, 102.3 mmol). The pH of the solution was adjusted to pH 4−5 by addition of acetic acid. Benzaldehyde (10.7 g, 97.7 mmol) was added. The solution was stirred at room temperature for 1 h, and the formation of the imine was monitored by MS. After complete formation of the imine, sodium cyanoborohydride (6.4 g, 102.3 mmol) was added. The resulting mixture was stirred at room temperature for 1 h. Formaldehyde (37% in H₂O, 24.9 mL, 334.4 mmol) was added, and the reaction mixture was stirred at room temperature for 45 min. The mixture was quenched with saturated aqueous sodium bicarbonate, and the organic solvent was evaporated under reduced pressure. The residue was extracted with ethyl acetate (3×). The combined organic layers were washed with brine, dried over magnesium sulfate, filtered, and concentrated. The crude was purified by flash chromatography (cyclohexane/ethyl acetate, 9:1) to afford (S)-2-(benzylmethylamino)-4-*tert*-butoxycarbonylaminobutyric acid methyl ester (**33**) (27.8 g, 82.6 mmol, 89%) as a colorless liquid. ^{1}H NMR (360 MHz, CDCl₃): δ 7.29−7.13 (m, 5H), 4.81 (br s, 1H), 3.70 (d, J = 13.0 Hz, 1H), 3.66 (s, 3H), 3.57 (d, J = 13 Hz, 1H), 3.29 (dd, J = 8.5, 6.7 Hz, 1H), 3.18−3.11 (m, 2H), 2.21 (s, 3H), 1.85−1.78 (m, 2H), 1.36 (s, 9 H). UPLC−MS m/z (ES⁺) (M + H)⁺ = 337.3. HRMS m/z (EI) (M + H)⁺ = 337.2123 (calcd for $C_{18}H_{29}N_2O_4$, 337.2127).

To a solution of **33** (9.00 g, 26.75 mmol) in methanol (270 mL) was added palladium hydroxide on carbon (20 wt % Pd, 0.50 g). The flask was evacuated and purged with hydrogen three times. The mixture was stirred under a hydrogen atmosphere (1 bar) overnight.

The flask was purged with argon. The mixture was diluted with dichloromethane and filtered over Celite. The filtrate was concentrated to afford **34** (6.60 g, 25.58 mmol, 96%) as a light yellow oil, which was used without further purification. ^{1}H NMR (360 MHz, CDCl$_3$): δ 5.25 (br s, 1H), 3.75 (s, 3H), 3.39−3.28 (m, 1H), 3.25−3.14 (m, 2H), 2.38 (s, 3H), 1.97−1.81 (m, 1H), 1.81−1.64 (m, 1H), 1.46 (s, 9 H). MS m/z (ES+) (M + H)$^+$ = 247.1.

(S)-2-{[3′-(4-Chloro-2,5-dimethylphenylsulfonylamino)-3,5-dimethylbiphenyl-4-carbonyl]methylamino}-4-dimethylami-nobutyric Acid Methyl Ester Hydrochloride (14). To a suspension of **21** (7.50 g, 16.92 mmol) in dichloromethane (250 mL) was added a catalytic amount of DMF followed by the dropwise addition of thionyl chloride (4.10 g, 2.50 mL, 34.46 mmol). The reation mixture was refluxed for 30 min, and a yellow solution was obtained. The mixture was concentrated under reduced pressure, and the residue was dried in vacuo for 15 min. To a solution of the residue in THF (250 mL) was added **34** (5.00 g, 20.30 mmol) followed by DIPEA (10.90 g, 14.7 mL, 84.40 mmol). The reaction mixture was stirred at room temperature overnight. The mixture was concentrated. The residue was taken up in EtOAc and washed with aqueous HCl (1 M, 2×), water (2×), saturated aqueous sodium bicarbonate (2×), and brine (2×). The organic layer was dried over magnesium sulfate, filtered, and concentrated. The residue was purified by flash chromatography (cyclohexane/ethyl acetate, 2:1) to afford (S)-2-{[3′-(4-chloro-2,5-dimethylphenylsulfonylamino)-3,5-dimethylbiphen-yl-4-carbonyl]methylamino}-4-*tert*-butoxycarbonylaminobutyric acid methyl ester (**35**) (9.18 g, 13.62 mmol, 80%) as an off-white solid. UPLC: rotamer A 6%, rotamer B 94%. ^{1}H NMR (360 MHz, CDCl$_3$): δ (ppm) 7.91 (s, 1H), 7.70 (s, 1H), 7.31−7.24 (m, 3H), 7.14 (s, 1H), 7.12−7.06 (m, 2H), 7.03 (dt, J = 6.5, 2.3 Hz, 1H), 5.55 (dd, J = 10.9, 4.4 Hz, 0.94H), 5.25 (br s, 1H), 4.59−4.54 (m, 0.06H), 3.82 (s, 2.82H), 3.76 (s, 0.18H), 3.66−3.43 (m, 1H), 3.17 (s, 0.18H), 3.11−2.98 (m, 1H), 2.79 (s, 2.82H), 2.62 (s, 3H), 2.37 (s, 6H), 2.36−2.29 (m, 3.94H), 2.25 (s, 0.06H), 2.07−2.01 (m, 1H), 1.47 (s, 9H). UPLC−MS m/z (ES$^+$) (M + H)$^+$ = 672.5. HRMS m/z (EI) (M + H)$^+$ = 672.2502 (calcd for C$_{34}$H$_{43}$ClN$_3$O$_7$S, 672.2510).

To a solution of **35** (6.00 g, 8.93 mmol) in dichloromethane (65 mL) was added HCl (2 M in diethyl ether, 44.6 mL, 89.20 mmol) dropwise. The reaction mixture was stirred at room temperature overnight, and a white precipitate was formed. The mixture was concentrated and the residue was dried in vacuo to afford (S)-2-{[3′-(4-chloro-2,5-dimethylphenylsulfonylamino)-3,5-dimethylbiphenyl-4-carbonyl]methylamino}-4-aminobutyric acid methyl ester hydro-chloride (**36**) (5.40 g, 8.93 mmol, quantitative) as an off-white solid. UPLC: rotamer A 5%, rotamer B 95%. ^{1}H NMR (360 MHz, DMSO-d_6): δ (ppm) 10.66 (s, 1H), 8.23 (br s, 3H), 8.00 (s, 1H), 7.50 (s, 1H), 7.36−7.28 (m, 3H), 7.19 (s, 2H), 7.10 (dt, J = 7.2, 1.9 Hz, 1H), 5.10 (dd, J = 9.7, 5.2 Hz, 1H), 3.73 (s, 3H), 3.07−2.91 (m, 1H), 2.91−2.78 (m, 1H), 2.75 (s, 3H), 2.55 (s, 3H), 2.47−2.38 (m, 1H), 2.36 (s, 3H), 2.27 (s, 3H), 2.26 (s, 3H), 2.25−2.16 (m, 1H). UPLC−MS m/z (ES$^+$) (M + H)$^+$ = 572.3. HRMS m/z (EI) (M + H)$^+$ = 572.1979 (calcd for C$_{29}$H$_{35}$ClN$_3$O$_5$S, 572.1986).

To a suspension of **36** (4.40 g, 7.23 mmol) in acetonitrile (79 mL) was added acetic acid (0.41 mL, 0.43 g, 7.23 mmol) followed by formaldehyde (37% in water, 5.40 mL, 72.52 mmol). The mixture was sonicated until a yellow solution was obtained. Sodium triacetoxybor-ohydride (4.90 g, 23.14 mmol) was added. The reaction mixture was stirred at room temperature for 40 min. The mixture was diluted with dichloromethane (360 mL) and washed with saturated aqueous sodium bicarbonate (2×) and water (2×). The organic layer was dried over magnesium sulfate, filtered, and concentrated. The residue was purified by flash chromatography (dichloromethane/methanol, 16:1) to afford a white solid, which was dissolved in dichloromethane and treated with an excess HCl (2 M in diethylether). The mixture was concentrated and the residue was dried in vacuo to provide **14** (2.40 g, 3.77 mmol, 52%) as a white solid. UPLC: rotamer A 7%, rotamer B 93%. ^{1}H NMR (360 MHz, DMSO-d_6): δ (ppm) 10.78 (br s, 1H), 10.64 (s, 1H), 8.00 (s, 1H), 7.51 (s, 1H), 7.37−7.28 (m, 3H), 7.23−7.18 (m, 2H), 7.09 (dt, J = 7.1, 2.0 Hz, 1 H), 5.15 (dd, J = 9.6, 5.3 Hz, 0.93H), 4.09−4.04 (m, 0.07H), 3.74 (s, 2.79H), 3.69 (s, 0.21H),

3.31−3.19 (m, 1H), 3.16 (s, 0.21H), 3.12−2.97 (m, 1H), 2.84−2.78 (m, 5.79H), 2.75 (s, 3H), 2.56 (s, 3H), 2.53−2.43 (m, 1H), 2.37 (s, 3H), 2.34−2.23 (m, 1H), 2.28 (s, 5.79H), 2.10 (s, 0.21H). UPLC−MS m/z (ES$^+$) (M + H)$^+$ = 600.3. HRMS m/z (EI) (M + H)$^+$ = 600.2291 (calcd for C$_{31}$H$_{39}$ClN$_3$O$_5$S, 600.2299).

(S)-2-{[3′-(4-Chloro-2,5-dimethylphenylsulfonylamino)-3,5-dimethylbiphenyl-4-carbonyl]methylamino}-4-dimethylami-nobutyric Acid Hydrochloride (15). To a solution of **14** (free base, 1.50 g, 2.50 mmol) in THF (70 mL) was added aqueous lithium hydroxide (1 M, 12.5 mL, 12.50 mmol). The reaction mixture was stirred at room temperature for 3 h. The mixture was acidified with aqueous HCl (1 M) to pH 3 and concentrated. The residue was purified by preparative HPLC (water/acetonitrile gradient) to give a white solid, which was taken up in dichloromethane and treated with an excess HCl (2 M in diethyl ether). The mixture was concentrated to afford **15** (0.94 g, 1.50 mmol, 60%) as a white solid. UPLC: rotamer A 4%, rotamer B 96%. ^{1}H NMR (360 MHz, DMSO-d_6): δ (ppm) 13.23 (br s, 1H), 10.63 (s, 1H), 10.60 (br s, 1H), 8.00 (s, 1H), 7.51 (s, 1H), 7.37−7.24 (m, 3H), 7.22−7.15 (m, 2H), 7.08 (dt, J = 7.1, 2.0 Hz, 1 H), 5.12 (dd, J = 9.9, 5.3 Hz, 1H), 3.30−3.19 (m, 1H), 3.09−2.97 (m, 1H), 2.81 (br s, 6H), 2.73 (s, 3H), 2.55 (s, 3H), 2.50−2.41 (m, 1H), 2.37 (s, 3H), 2.30−2.24 (m, 1H), 2.28 (s, 6H). UPLC−MS m/z (ES$^+$) (M + H)$^+$ = 586.3. HRMS m/z (EI) (M + H)$^+$ = 586.2133 (calcd for C$_{30}$H$_{37}$ClN$_3$O$_5$S, 586.2142).

■ ASSOCIATED CONTENT

Ⓢ Supporting Information

Determination of K_D for **15** by Schild plot analysis and synthesis procedures and spectral data for compounds **5−13, 16−18, 27, 28,** and **30−32**. This material is available free of charge via the Internet at http://pubs.acs.org.

■ AUTHOR INFORMATION

Corresponding Author
*Phone: +41 61 3246858. E-mail: daniela.angst@novartis.com.
Notes
The authors declare no competing financial interest.

■ ACKNOWLEDGMENTS

■ ABBREVIATIONS USED

CAV, cardiac allograft vasculopathy; DA, Dark Agouti; EBD, Evans blue dye; GTPγ^{35}S, [^{35}S]guanosine 5′-O-(3-thiotriphos-phate); MST, median survival time; PBL, peripheral blood lymphocyte; S1P, sphingosine 1-phosphate

■ REFERENCES

(1) Sanchez, T.; Hla, T. Structural and functional characteristics of S1P receptors. *J. Cell. Biochem.* **2004**, *92*, 913−922.

(2) Brinkmann, V. Sphingosine 1-phosphate receptors in health and disease: mechanistic insights from gene deletion studies and reverse pharmacology. *Pharmacol. Ther.* **2007**, *115*, 84−105.

(3) Rivera, J.; Proia, R. L.; Olivera, A. The alliance of sphingosine-1-phosphate and its receptors in immunity. *Nat. Rev. Immunol.* **2008**, *8*, 753−763.

(4) Matloubian, M.; Lo, C. G.; Cinamon, G.; Lesneski, M. J.; Xu, Y.; Brinkmann, V.; Allende, M. L.; Proia, R. L.; Cyster, J. G. Lymphocyte egress from thymus and peripheral lymphoid organs is dependent on S1P receptor 1. *Nature* **2004**, *427*, 355−360.

(5) Tarrasón, G.; Aulí, M.; Mustafa, S.; Dolgachev, V.; Domènech, M. T.; Prats, N.; Domínguez, M.; López, R.; Aguilar, N.; Calbet, M.; Pont, M.; Milligan, G.; Kundel, S. L.; Godessart, N. The sphingosine-1-phosphate receptor-1 antagonist, W146, causes early and short-lasting

peripheral blood lymphopenia in mice. *Int. Immunopharmacol.* **2011**, *11*, 1773−1779.

(6) Fujii, Y.; Ohtake, H.; Ono, N.; Hara, T.; Sakurai, T.; Takahashi, S.; Takayama, T.; Fukasawa, Y.; Shiozawa, F.; Tsukahara, N.; Hirayama, T.; Igarashi, Y.; Goitsuka, R. Lymphopenia induced by a novel selective S1P$_1$ antagonist structurally unrelated to S1P. *Biochim. Biophys. Acta* **2012**, *1821*, 600−606.

(7) Berst, F.; Grosche, P.; Janser, P.; Zecri, F.; Bollbuck, B. *N*-Biaryl (Hetero) Arylsulphonamide Derivatives Useful in the Treatment of Diseases Mediated by Lymphocytes Interactions. PCT Int. Appl. WO 2008/028937, 2008.

(8) Pan, S.; Mi, Y.; Pally, C.; Beerli, C.; Chen, A.; Guerini, D.; Hinterding, K.; Nuesslein-Hildesheim, B.; Tuntland, T.; Lefebvre, S.; Liu, Y.; Gao, W.; Chu, A.; Brinkmann, V.; Bruns, C.; Streiff, M.; Cannet, C.; Cooke, N.; Gray, N. A monoselective sphingosine-1-phosphate receptor-1 agonist prevents allograft rejection in a stringent rat heart transplantation model. *Chem. Biol.* **2006**, *13*, 1227−1234.

(9) Chiba, K. Sphingosine 1-phosphate receptor type 1 as a novel target for the therapy of autoimmune diseases. *Inflammation Regener.* **2010**, *10*, 160−168.

(10) Chiba, K.; Kataoka, H.; Maeda, Y.; Seki, N.; Sugahara, K. Sphingosine 1-phosphate receptor modulator, fingolimod (FTY720), provides a new therapeutic approach for autoimmune diseases. *Inflammation Regener.* **2010**, *30*, 419−424.

(11) Saha, A. K.; Yu, X.; Lin, J.; Lobera, M.; Sharadendu, A.; Chereku, S.; Schutz, N.; Segal, D.; Marantz, Y.; McCauley, D.; Middleton, S.; Siu, J.; Bürli, R. W.; Buys, J.; Horner, M.; Salyers, K.; Schrag, M.; Vargas, H. M.; Xu, Y.; McElvain, M.; Xu, H. Benzofuran derivatives as potent, orally active S1P$_1$ receptor agonists: a preclinical lead molecule for MS. *ACS Med. Chem. Lett.* **2011**, *2*, 97−101.

(12) Nishi, T.; Miyazaki, S.; Takemoto, T.; Suzuki, K.; Iio, Y.; Nakajima, K.; Ohnuki, T.; Kawase, Y.; Nara, F.; Inaba, S.; Izumi, T.; Yuita, H.; Oshima, K.; Doi, H.; Inoue, R.; Tomisato, W.; Kagari, T.; Shimozato, T. Discovery of CS-0777: a potent, selective, and orally active S1P$_1$ agonist. *ACS Med. Chem. Lett.* **2011**, *2*, 368−372.

(13) Piali, L.; Froidevaux, S.; Hess, P.; Nayler, O.; Bolli, M. H.; Schlosser, E.; Kohl, C.; Steiner, B.; Clozel, M. The selective sphingosine 1-phosphate receptor 1 agonist ponesimod protects against lymphocyte-mediated tissue inflammation. *J. Pharmacol. Exp. Ther.* **2011**, *337*, 547−556.

(14) Brinkmann, V.; Billich, A.; Baumruker, T.; Heining, P.; Schmouder, R.; Francis, G.; Aradhye, S.; Burtin, P. Fingolimod (FTY720): discovery and development of an oral drug to treat multiple sclerosis. *Nat. Rev. Drug Discovery* **2010**, *9*, 883−897.

(15) Fujii, Y.; Hirayama, T.; Ohtake, H.; Ono, N.; Inoue, T.; Sakurai, T.; Takayama, T.; Matsumoto, K.; Tsukahara, N.; Hidano, S.; Harima, N.; Nakazawa, K.; Igarashi, Y.; Goitsuka, R. Amelioration of collagen-induced arthritis by a novel S1P$_1$ antagonist with immunomodulatory activities. *J. Immunol.* **2012**, *188*, 206−215.

(16) Fujii, Y.; Ueda, Y.; Ohtake, H.; Ono, N.; Takayama, T.; Nakazawa, K.; Igarashi, Y.; Goitsuka, R. Blocking S1P interaction with S1P$_1$ receptor by a novel competitive S1P$_1$-selective antagonist inhibits angiogenesis. *Biochem. Biophys. Res. Commun.* **2012**, *419*, 754−760.

(17) Ibrahim, M. A.; Johnson, H. W. B.; Won Jeong, J.; Lewis, G. L.; Shi, X.; Noguchi, R. T.; Williams, M.; Leahy, J. W.; Nuss, J. M.; Woolfrey, J.; Banica, M.; Bentzien, F.; Chou, Y.-C.; Gibson, A.; Heald, N.; Lamb, P.; Mattheakis, L.; Matthews, D.; Shipway, A.; Wu, X.; Zhang, W.; Zhou, S.; Shankar, G. Discovery of a novel class of potent and orally bioavailable sphingosine 1-phosphate receptor 1 antagonists. *J. Med. Chem.* **2012**, *55*, 1368−1381.

(18) Quancard, J.; Bollbuck, B.; Janser, P.; Angst, D.; Berst, F.; Buehlmayer, P.; Streiff, M.; Beerli, C.; Brinkmann, V.; Guerini, D.; Smith, P. A.; Seabrook, T.; Traebert, M.; Seuwen, K.; Hersperger, R.; Bruns, C.; Bassilana, F.; Bigaud, M. A potent and selective S1P$_1$ antagonist with efficacy in experimental autoimmune encephalomyelitis. *Chem. Biol.* **2012**, *19*, 1142−1151.

(19) Ertl, P.; Rohde, B.; Selzer, P. Fast calculation of molecular polar surface area as a sum of fragment-based contributions and its application to the prediction of drug transport properties. *J. Med. Chem.* **2000**, *43*, 3714−3717.

(20) Beaumont, K.; Webster, R.; Gardner, I.; Dack, K. Design of ester prodrugs to enhance oral absorption of poorly permeable compounds: challenges to the discovery scientist. *Curr. Drug Metab.* **2003**, *4*, 461−485.

(21) Liederer, B. M.; Borchardt, R. T. Enzymes involved in the bioconversion of ester-based prodrugs. *J. Pharm. Sci.* **2006**, *95*, 1177−1195.

(22) Smith, D. A. Do prodrugs deliver? *Curr. Opin. Drug Discovery Dev.* **2007**, *10*, 550−559.

(23) Oo, M. L.; Thangada, S.; Wu, M.-T.; Liu, C. H.; Macdonald, T. L.; Lynch, K. R.; Lin, C.-Y.; Hla, T. Immunosuppressive and anti-angiogenic sphingosine 1-phosphate receptor-1 agonists induce ubiquitinylation and proteasomal degradation of the receptor. *J. Biol. Chem.* **2007**, *282*, 9082−9089.

(24) Oo, M. L.; Chang, S.-H.; Thangada, S.; Wu, M.-T.; Rezaul, K.; Blaho, V.; Hwang, S.-I.; Han, D. K.; Hla, T. Engagement of S1P$_1$-degradative mechanisms leads to vascular leak in mice. *J. Clin. Invest.* **2011**, *121*, 2290−2300.

(25) Koyrakh, L.; Roman, M. I.; Brinkmann, V.; Wickman, K. The heart rate decrease caused by acute FTY720 administration is mediated by the G protein-gated potassium channel I$_{KACh}$. *Am. J. Tranplant.* **2005**, *5*, 529−536.

(26) Gergely, P.; Nuesslein-Hildesheim, B.; Guerini, D.; Brinkmann, V.; Traebert, M.; Bruns, C.; Pan, S.; Gray, N. S.; Hinterding, K.; Cooke, N. G.; Groenewegen, A.; Vitaliti, A.; Sing, T.; Luttringer, O.; Yang, J.; Gardin, A.; Wang, N.; Crumb, W. J.; Saltzman, M.; Rosenberg, M.; Wallström, E. The selective S1P receptor modulator BAF312 redirects lymphocyte distribution and has species-specific effects on heart rate. *Br. J. Pharmacol.* **2012**, *167*, 1035−1037.

(27) Sanna, M. G.; Liao, J.; Jo, E.; Alfonso, C.; Ahn, M.-Y.; Peterson, M. S.; Webb, B.; Lefebvre, S.; Chun, J.; Gray, N.; Rosen, H. Sphingosine 1-phosphate (S1P) receptor subtypes S1P$_1$ and S1P$_3$, respectively, regulate lymphocyte recirculation and heart rate. *J. Biol. Chem.* **2004**, *279*, 13839−13848.

(28) Pretsch, E.; Bühlmann, P.; Badertscher, M. *Spektroskopische Daten zur Strukturaufklärung Organischer Verbindungen*, 5th ed.; Springer: Heidelberg, Germany, 2010; pp 135−136, 224−226.

(29) Gate, E. N.; Hooper, D. L.; Stevens, M. F. G.; Threadgill, M. D.; Vaughan, K. ^{1}H and ^{13}C NMR spectra of the rotational isomers of *N*-hydroxymethylamides and derivatives. *Magn. Reson. Chem.* **1985**, *23*, 78−82.

(30) Sanna, M. G.; Wang, S.-K.; Gonzalez-Cabrera, P. J.; Don, A.; Marsolais, D.; Matheu, M. P.; Wei, S. H.; Parker, I.; Jo, E.; Cheng, W.-C.; Cahalan, M. D.; Wong, C.-H.; Rosen, H. Enhancement of capillary leakage and restoration of lymphocyte egress by a chiral S1P$_1$ antagonist in vivo. *Nat. Chem. Biol.* **2006**, *2*, 434−441.

(31) Evenou, J. P.; Wagner, J.; Zenke, G.; Brinkmann, V.; Wagner, K.; Kovarik, J.; Welzenbach, K. A.; Weitz-Schmidt, G.; Guntermann, C.; Towbin, H.; Cottens, S.; Kaminski, S.; Letschka, T.; Lutz-Nicoladoni, C.; Gruber, T.; Hermann-Kleiter, N.; Thuille, N.; Baier, G. The potent protein kinase C-selective inhibitor AEB071 (sotrastaurin) represents a new class of immunosuppressive agents affecting early T-cell activation. *J. Pharmacol. Exp. Ther.* **2009**, *330*, 792−801.

(32) Schuler, W.; Sedrani, R.; Cottens, S.; Häberlin, B.; Schulz, M.; Schuurman, H.-J.; Zenke, G.; Zerwes, H.-G.; Schreier, M. H. SDZ RAD, a new rapamycin derivative: pharmacological properties in vitro and in vivo. *Transplantation* **1997**, *64*, 36−42.

(33) Weckbecker, G.; Pally, C.; Beerli, C.; Burkhart, C.; Wieczorek, G.; Metzler, B.; Morris, R. E.; Wagner, J.; Bruns, C. Effects of the novel protein kinase C inhibitor AEB071 (sotrastaurin) on rat cardiac allograft survival using single agent treatment or combination therapy with cyclosporin, everolimus or FTY720. *Tranplant. Int.* **2010**, *23*, 543−552.

(34) Brinkmann, V.; Chen, S.; Feng, L.; Pinschewer, D.; Nikolova, Z.; Hof, R. FTY720 alters lymphocyte homing and protects allografts without inducing general immunosuppression. *Tranplant. Proc.* **2001**, *33*, 530−531.

(35) Zaragoza, F.; Stephensen, H. (Cyanomethyl)-trialkylphosphonium iodides: efficient reagents for the intermolecular alkylation of amines with alcohols in solution and on solid phase. *J. Org. Chem.* **2001**, *66*, 2518−2521.

(36) Ono, K.; Lindsey, E. S. Improved technique of heart transplantation in rats. *J. Thorac. Cardiovasc. Surg.* **1969**, *57*, 225−229.

(37) Stewart, S.; Winters, G. L.; Fishbein, M. C.; Tazelaar, H. D.; Kobashigawa, J.; Abrams, J.; Andersen, C. B.; Angelini, A.; Berry, G. J.; Burke, M. M.; Demetris, A. J.; Hammond, E.; Itescu, S.; Marboe, C. C.; McManus, B.; Reed, E. F.; Reinsmoen, N. L.; Rodriguez, E. R.; Rose, A. G.; Rose, M.; Suciu-Focia, N.; Zeevi, A.; Billingham, M. E. Revision of the 1990 working formulation for the standardization of nomenclature in the diagnosis of heart rejection. *J. Heart Lung Transplant.* **2005**, *24*, 1710−1720.